

Original Article

Pharmacokinetic/pharmacodynamic studies on exenatide in diabetic rats

Xin-gang LI², Liang LI², Xuan ZHOU², Ye CHEN², Yu-peng REN², Tian-yan ZHOU^{1,2,*}, Wei LU^{1,2,*}

¹State Key Laboratory of Natural and Biomimetic Drugs (Peking University), Beijing 100191, China; ²Department of Pharmaceutics, School of Pharmaceutical Sciences, Peking University Health Science Center, Beijing 100191, China

Aim: To quantitatively evaluate the blood glucose-lowering effect of exenatide in diabetic rats.

Methods: Male Harlan-Sprague-Dawley rats were treated with high-fat diet/streptozotocin to induce type 2 diabetes. After subcutaneous administration of a single dose of exenatide (4.2, 42, or 210 µg/kg), serum exenatide, insulin concentration and blood glucose were measured. The pharmacokinetics of exenatide was characterized by a two-compartment model with first-order absorption. Insulin turnover was characterized by an effect compartment and indirect response combined model. Glucose turnover was described using an indirect response model with insulin (in effect compartment) stimulating glucose disposition and insulin (in insulin compartment) inhibiting glucose production simultaneously. The model parameters were estimated using nonlinear mixed-effects model program. Visual predictive check and model evaluation were used to make assessments.

Results: Exenatide exhibited rapid absorption with $k_a=4.45\text{ h}^{-1}$, and the two-compartment model well described its pharmacokinetic profile. For the pharmacodynamic model, exenatide increased insulin release with the estimated S_{m1} of 0.822 and SC_{50} of 4.02 µg/L. It was demonstrated that insulin stimulated glucose dissipation ($S_{m2}=0.0513$) and inhibited the production of glucose ($I_m=0.0381$). Visual predictive check and model evaluation study indicated that a credible model was developed.

Conclusion: The glucose-lowering effect of exenatide in diabetic rats is reliably described and predicted by the combined effect compartment/indirect response model.

Keywords: exenatide; type 2 diabetes; insulin; glucose; pharmacokinetic/pharmacodynamic; effect compartment; indirect response model; NONMEM

Acta Pharmacologica Sinica (2012) 33: 1379–1386; doi: 10.1038/aps.2012.33; published online 4 Jun 2012

Introduction

Diabetes mellitus is a major health risk in many countries, and the incidence rates are increasing. Type 2 diabetes accounts for more than 90% of all diabetes, and the pathogenesis is characterized by peripheral insulin resistance and progressive failure of pancreatic β -cell function, ultimately resulting in deficient insulin secretion^[1]. Various anti-diabetic agents that function via different mechanisms have been developed and used in clinical practice. Incretin-based therapies slow down the natural decline in insulin production, which enable it to be used widely for type 2 diabetes^[2]. Glucagon-like peptide (GLP)-1 is an incretin hormone secreted by intestinal mucosa in response to meal ingestion. Physiologic GLP-1 exhibits several gluco-regulatory functions, such as glucose-dependent

enhancement of insulin secretion, slowing down gastric emptying to modulate nutrient absorption, reduction of food intake and body weight, increase in β -cell mass (animal studies), and enhancement of β -cell function^[3–7].

However, GLP-1 has an extremely short half-life (0.8–4.7 min) in plasma^[4]. Exenatide is a 39-amino acid amidated peptide incretin mimetic that shares gluco-regulatory activities with the GLP-1^[8]. Acute and chronic administration of exenatide was shown to exert anti-diabetic effects in several animal models of type 2 diabetes^[9]. Several pharmacokinetic/pharmacodynamic (PK/PD) models of exenatide in diabetes mellitus have been developed to evaluate its efficacy. A physiologic pharmacodynamic model of exenatide was established to evaluate the effects on glucose and insulin regulation in both healthy and type 2 diabetic subjects. However, drug concentrations were unavailable during the modeling process, and only hypothetical pharmacokinetic driving functions were used^[10]. Using rats as an experimental model to assess the pharmacodynamic of exenatide was addressed by Jusko *et al*,

* To whom correspondence should be addressed.
E-mail Luwei_pk@bjmu.edu.cn (Wei LU);
tianyanzhou@bjmu.edu.cn (Tian-yan ZHOU)
Received 2012-02-07 Accepted 2012-03-12

and a mechanism-based PK/PD model of exenatide in type 2 diabetic Goto-Kakizaki rats was proposed^[11]. Acute hyperglycemia, a novel aspect of exenatide action was incorporated into their final model. Jusko's findings raise important considerations for investigating the acute glycemic effect of exenatide in diabetic rats.

In this study, a PK/PD model based on the insulinotropic effect of exenatide was developed in streptozotocin (STZ)-induced type 2 diabetic rats. The objective of the current study was to characterize the relationships among serum exenatide, serum insulin, and blood glucose in type 2 diabetic rats based on the establishment of a mechanism-based model. The final model was assessed by visual predictive check (VPC) and external validation.

Materials and methods

Materials

Exenatide was purchased from Taishi Biotechnology Co, Ltd (Shanghai, China). Exenatide enzyme immunoassay (EIA) kits were purchased from Phoenix Pharmaceuticals, Inc (CA, USA). Streptozotocin (STZ) was obtained from Sigma (Sigma, MO, USA). The insulin ELISA kit was purchased from Groundwork Biotechnology Diagnostic Ltd (CA, USA).

Induction of experimental diabetes in rats

Male Harlan-Sprague-Dawley rats (HSD), seven weeks of age, and weighing approximately 200 g, were obtained from the Experimental Animal Center at Peking University Health Science Center, Beijing. All experiments were carried out following the Guide for Care and Use of Laboratory Animals as adopted and promulgated by the Animal Ethics Committee of the Peking University Health Science Center. All rats were maintained on a 12/12-h light/dark cycle and at an ambient temperature of 20–25 °C. After one week of acclimation, animals were fed a high-fat diet consisting of 10% lard, 20% sucrose, 2% cholesterol, 1% cholate, and 67% normal chow diet (Keaoxili Fodder Co Ltd Beijing, China). All rats were allowed to eat and drink water *ad libitum*. After eight weeks of the high-fat diet, rats were fasted for 12 h (with free access to water) and each rat was injected intraperitoneally with 45 mg/kg STZ in 0.1 mol/L citric acid buffer (pH 4.3). Three weeks after the injection, rats were fasted for 12 h (with free access to water) before their blood glucose was measured by glucometer (ACCU-CHEK, Advantage, Germany)^[12]. Rats with fasting blood glucose above 16.7 mmol/L were considered to be diabetic.

Regimen design

Twenty-four rats that had developed type 2 diabetes, weighing 300–350 g, were randomly divided into four experimental groups and received sc administration of 0, 4.2, 42, or 210 µg/kg of exenatide, respectively. Exenatide was diluted immediately before injection using acetate buffer (pH 4.0). Before drug administration, all of the rats were fasted for two hours. The rats in the control group received a single sc injection of the acetate buffer. Sampling time was determined

based on previous pilot pharmacokinetic and pharmacodynamic studies. At the scheduled time after administration (Table 1), a blood sample (about 0.25 mL) was collected via the retro-orbital sinus, and blood glucose was measured simultaneously with a glucometer. The sera were separated by centrifugation (8500×g, 5 min) and then frozen at -70 °C until analyzed for exenatide and insulin.

Table 1. The sampling time under different doses.

Dose (µg/kg)	Schedule time (h)											
0	0	0.25	0.5	1	2	4	6	8	12	16	24	
4.2	0	0.25	0.5	1	2	4	6	8				
42	0	0.25	0.5	1	2	4	6	8	12	16		
210	0	0.25	0.5	1	2	4	6	8	12	16	24	

Experimental procedures

Serum exenatide concentrations in type 2 diabetic rats were measured using a commercial Exenatide EIA kit. The calibration curve was linear over the concentration range of 0.08–0.86 µg/L. The lower limit of quantification was 0.1 µg/L and the serum samples with exenatide concentrations >0.86 µg/L were diluted with assay buffer provided by the manufacturer and were subsequently analyzed. Serum concentrations of insulin were measured using rat insulin ELISA kits. General procedures followed the manufacturer's instructions. Plates were read at OD₄₅₀ on an enzyme-linked immunosorbent assay plate reader (BIO-RAD, USA).

Data analysis

A population approach was applied to investigate the pharmacokinetics and pharmacodynamics of exenatide. The data from all individuals at different dose levels were fitted simultaneously. All fittings and simulations were conducted using the program nonlinear mixed effect model (NONMEM, Version 7.2, ICON Development Solution, USA) by first-order conditional estimation with interaction.

Inter-individual variability on these parameters was modeled according to an exponential equation, based on the assumption that the parameters are log-normally distributed.

$$p_i = \theta \cdot \exp(\eta_i) \quad (1)$$

where θ is the population typical value for parameter P . P_i is individual i 's value and $\exp(\eta_i)$ is the random deviation of P_i from P . The value for η_i was assumed to be independently and normally distributed with a mean of zero and variance ω^2 .

Residual error was characterized by combining the proportional and additive error models as follows.

$$C_{ij} = C_{ij}^P \cdot (1 + \varepsilon_{1ij}) + \varepsilon_{2ij} \quad (2)$$

where C_{ij} and C_{ij}^P are the observed and predicted in i th individual's j th serum concentration, respectively, and ε_{1ij} and ε_{2ij} account for the proportional and additive intra-individual

errors, which are assumed to be normally distributed with a mean of zero and variances of σ_1^2 and σ_2^2 , respectively.

Pharmacokinetic model

A set of differential equations in a two-compartment model with first-order absorption was used to describe the change in drug concentration in each compartment (Figure 1).

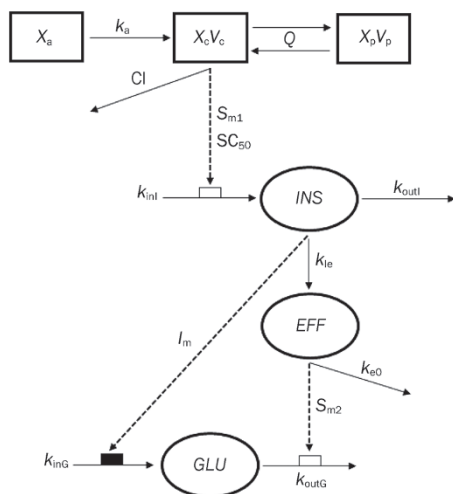


Figure 1. Schematic representation of the combined effect compartment/indirect response pharmacokinetic/pharmacodynamic model for describing the hypoglycemic effect of exenatide after sc administration in diabetic rats. Black rectangle: inhibition, white rectangle: stimulation. Continuous lines denote fluxes of mass and dotted lines indicate control fluxes. Insulin is separated into two compartments: one compartment is in blood (insulin compartment) and the other is in muscle and adipose (effect compartment). Blood insulin inhibits glucose production by decreasing gluconeogenesis and glycogenolysis; meanwhile, insulin in the effect compartment stimulates glucose dissipation by increasing cellular intake of glucose.

$$\frac{dX_a}{dt} = -k_a \cdot X_a \quad (3)$$

$$\frac{dX_c}{dt} = k_a \cdot X_a - Cl \cdot C_c - Q \cdot (C_c - C_p) \quad (4)$$

$$\frac{dX_p}{dt} = Q \cdot (C_c - C_p) \quad (5)$$

where k_a is the first-order absorption rate constant. Exenatide in the central compartment (X_c : amount of exenatide in central compartment) is distributed to and from the peripheral compartment (X_p : amount of exenatide in peripheral compartment) with the same inter-compartment clearance (Q), and is eliminated with system clearance (Cl). Serum exenatide concentration (C_c) and peripheral compartment exenatide concentration (C_p) were calculated as follows:

$$C_c = \frac{X_c}{V_c} \quad (6)$$

$$C_p = \frac{X_p}{V_p} \quad (7)$$

where V_c and V_p are apparent volume of distribution in the central and peripheral compartments, respectively.

Pharmacodynamic model

Based on the insulinotropic effect of exenatide^[8] and glucose-lowering effect of insulin, the relationship among serum exenatide, serum insulin, and glucose-lowering effect was fitted using an integral PK/PD model (Figure 1). The insulin and blood glucose were produced with a zero-order input rate and dissipated with a first-order output rate. According to the insulinotropic effect of exenatide, this stimulation of the input rate of insulin (INS) by exenatide is described by the following equations:

$$\frac{dINS}{dt} = k_{inI} \cdot \left(1 + \frac{S_{m1} \cdot C}{SC_{50} + C}\right) - k_{outI} \cdot INS \quad (8)$$

$$INS_0 = \frac{k_{inI}}{k_{outI}} \quad (9)$$

where k_{inI} is the zero-order input rate constant and k_{outI} is the first-order output rate constant. S_{m1} and SC_{50} are the drug-specific parameters representing the maximal stimulation and the exenatide concentration required for half-maximal stimulation, respectively. INS_0 represents the basal level of insulin when there is no drug *in vivo*.

Sites of action for insulin are mainly located in liver, muscle and adipose. Liver has a robust blood supply and insulin equilibrium can be reached quickly between blood and liver, such that liver and blood were treated as a single compartment, *ie*, the insulin compartment in the pharmacodynamic model (Figure 1). It is assumed that insulin in the insulin compartment can act directly on its corresponding receptors located in liver. However, the lack of the same robust blood supply in muscle and adipose tissue results in a distributional delay for insulin. So, an effect compartment was employed in the pharmacodynamic model to imitate muscle and adipose tissue (Figure 1). Briefly, the effect compartment is assumed to be a separate compartment that directly connects to the insulin compartment by a first-order rate process (k_{ie}). The elimination of insulin from the effect compartment is also characterized by a first-order rate process (k_{e0}). A differential equation entailing the insulin level in the effect compartment (INS_e) is described as follow:

$$\frac{dINS_e}{dt} = k_{e0} \cdot (INS - INS_e) \quad (10)$$

Before exenatide injection, there was no change in INS_e , therefore,

$$INS_{e,0} = INS_0 \quad (11)$$

where $INS_{e,0}$ is the insulin basal value in the effect compartment.

Due to fasting, the level of blood glucose is reduced as time goes on, both in treatment and control groups. To minimize the interference of fasting on blood glucose, the effect of exenatide (EOE) on glucose was normalized as follows:

$$EOE = \frac{GLU_{it}^T / GLU_{i0}^T}{GLU_{it}^C / GLU_{i0}^C} \quad (12)$$

where GLU_{i0}^T/GLU_{it}^T refer to blood glucose level of *i*th rat at time 0 and time *t* in the treatment group, while GLU_o^C/GLU_t^C represent the relevant average levels in the control group, respectively. The *EOE* values are between 0 and 1.

As we know, insulin exhibits multiple gluco-regulatory functions by inhibiting inputs such as gluconeogenesis and glycogenolysis, as well as by stimulating outputs such as glucose uptake into muscle and adipose tissues. The change of *EOE* is described in the following equation.

$$\frac{dEOE}{dt} = k_{inG} \cdot [1 - I_m \cdot (INS - INS_0)] - k_{outG} \cdot [1 + S_{m2} \cdot (INS_e - INS_{e0})] \cdot EOE \quad (13)$$

where I_m and S_{m2} are the inhibitory and stimulatory factors with first-order kinetics, respectively. The *EOE* starts from the basal value EOE_0 , then changes with time following exenatide administration, and eventually returns to EOE_0 .

$$EOE_0 = \frac{k_{inG}}{k_{outG}} \quad (14)$$

Normalization transformed all the rats' EOE_0 into 1, so

$$k_{inG} = k_{outG} \quad (15)$$

A three-step approach was applied to establish the PK/PD linked model, by which individual estimates were first obtained from the pharmacokinetic parameters. In the second step, the parameters of insulinotropic effect of exenatide were estimated with fixed pharmacokinetic parameters. Finally, the parameters of the glucose-lowering effect of insulin were estimated. In this way we could avoid biases in the pharmacokinetic data which could interfere with the estimation of the pharmacodynamic parameters and vice versa. In addition, both the effect compartment and indirect response model were integrated to describe the PK/PD model, which was defined as combined effect compartment/indirect response model.

Model validation

We used both visual predictive check (VPC) and external test for model validation in this study. VPC is based on a graphical comparison between the observed data and prediction intervals derived from the simulated data. Based on the typical values of the PK and PK/PD parameters obtained from the final model, the exenatide concentrations, insulin levels and *EOE* for all dose regimens were simulated for 2000 times using NONMEM software. The observed data were graphically overlaid with the median values along with the 5th and 95th percentiles from the simulated data. The model was deemed adequate if the observed data were appropriately distributed within the 5th and 95th percentiles of the simulated data.

To externally validate the predictability of our PK/PD model, a model evaluation study was also performed. Another 10 rats were randomly divided into two groups for sc administration of 0 µg/rat (acetate buffer) or 21 µg/rat exenatide. The blood glucose was determined at 0 (pre-dose), 2, 4, 6, 8, 12, and 15 h. The observed data were used to be compared with the predicted data which simulated from our

final PK/PD model with all model parameters were fixed to their typical values.

Results

Pharmacokinetics

A two-compartment with first-order absorption model captured the overall profiles of serum exenatide at each dose level very well. The profiles of serum exenatide concentrations after sc administration were shown in Figure 2A–2C. Exenatide was absorbed rapidly ($k_a=4.45 \text{ h}^{-1}$) and achieved a maximum concentration at about half an hour after sc injection. The VPC showed that the final pharmacokinetic model could predict closely the time-course of exenatide in rats (Figure 2A'–2C'), except for several exenatide concentrations that were under-predicted by the model. 5.76% of the observed concentrations fell outside the 90% prediction intervals (PI).

The estimates of pharmacokinetic parameters are summarized in Table 2. All parameters were estimated with good precision (RSE% < 30.0%) and comparable to prior reports^[4, 13]. The analysis of variance for clearance (Cl) and apparent central volume of distribution (V_c) showed no statistical differences ($P > 0.05$) among different dose levels. The results indicated that the pharmacokinetics of exenatide was linear, and the parameters were dose-independent from 4.2 to 210 µg/kg.

Table 2. Parameter estimates obtained from the time profiles of exenatide after administration to diabetic rats using the two-compartment pharmacokinetic model.

Parameter ^a	Estimate (RSE%) ^b	CV% ^c
k_a (h^{-1})	4.45 (12.3)	38.3
Cl/F (L/h)	0.198 (6.46)	27.7
V_c /F (L)	0.397 (8.82)	30.1
Q/F (L/h)	0.086 (18.6)	64.9
V_p /F (L)	1.18 (27.0)	82.2
Residual error		
σ_1 (Proportional, CV%)	0 (Fix)	
σ_2 (Additive, SD)	0.179 µg/L	

^a k_a , absorption rate constant; Q/F, inter-compartmental clearance; V_c /F, central volume of distribution; Cl/F, central clearance; V_p /F, peripheral volume of distribution.

^b RSE=relative standard error.

^c CV=coefficient of variation.

Pharmacodynamics

The plots of observed and predicted serum insulin concentrations versus time are shown in Figure 3A–3C. The indirect response model captured the change in insulin profile well. Baseline insulin was $10.116 \pm 3.845 \text{ mU/L}$ ($P > 0.05$ among groups). Serum insulin increased at all exenatide doses and reached a peak at about 1 h (4.2 µg/kg), 1–2 h (42 µg/kg), and 2 h (210 µg/kg); and the peak insulin concentrations were not significantly different among groups ($P > 0.05$). The time-delay between serum exenatide and insulin could be observed

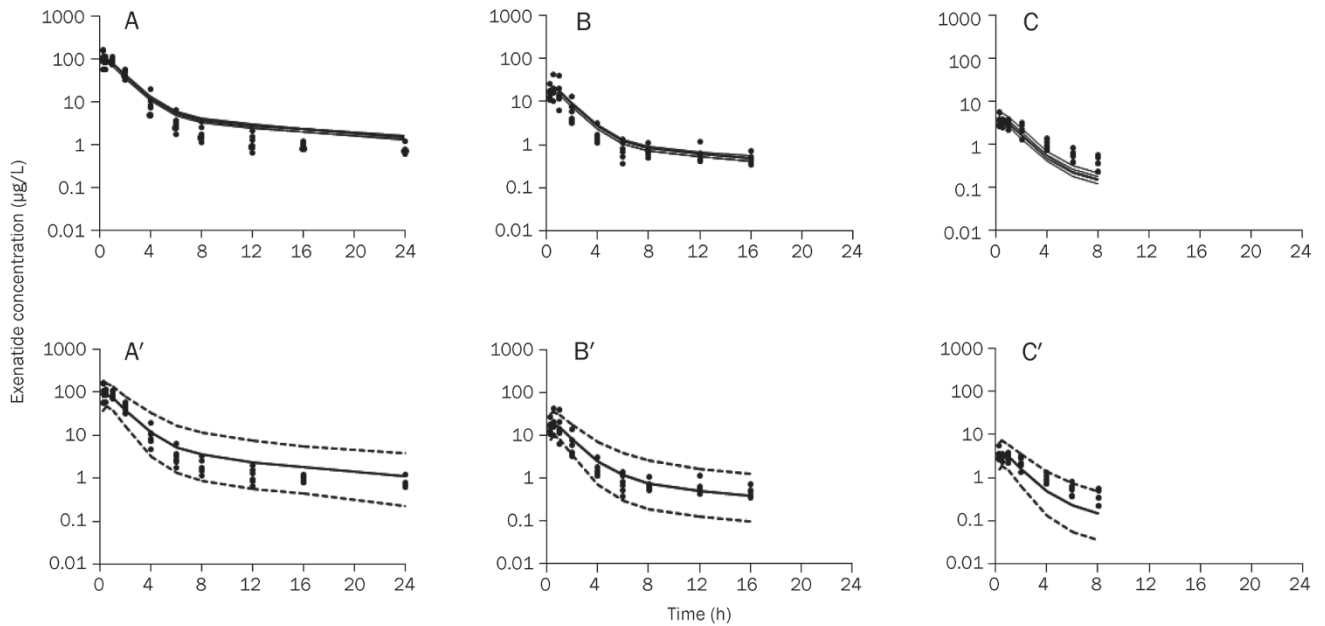


Figure 2. Observed and predicted serum exenatide concentrations-time profiles after a single administration of exenatide at the dose of 210 (A), 42 (B), and 4.2 $\mu\text{g}/\text{kg}$ (C) in diabetic rats. The solid dots represent individual data from rats and the solid lines represent the model fit lines. Visual predictive check of serum exenatide concentration-time profiles after single administrations of exenatide at the dose of 210 (A'), 42 (B'), and 4.2 $\mu\text{g}/\text{kg}$ (C'). The ranges between the dotted lines depict the 90% prediction intervals. The solid lines present the medians of simulated data. The solid dots are the observed concentrations.

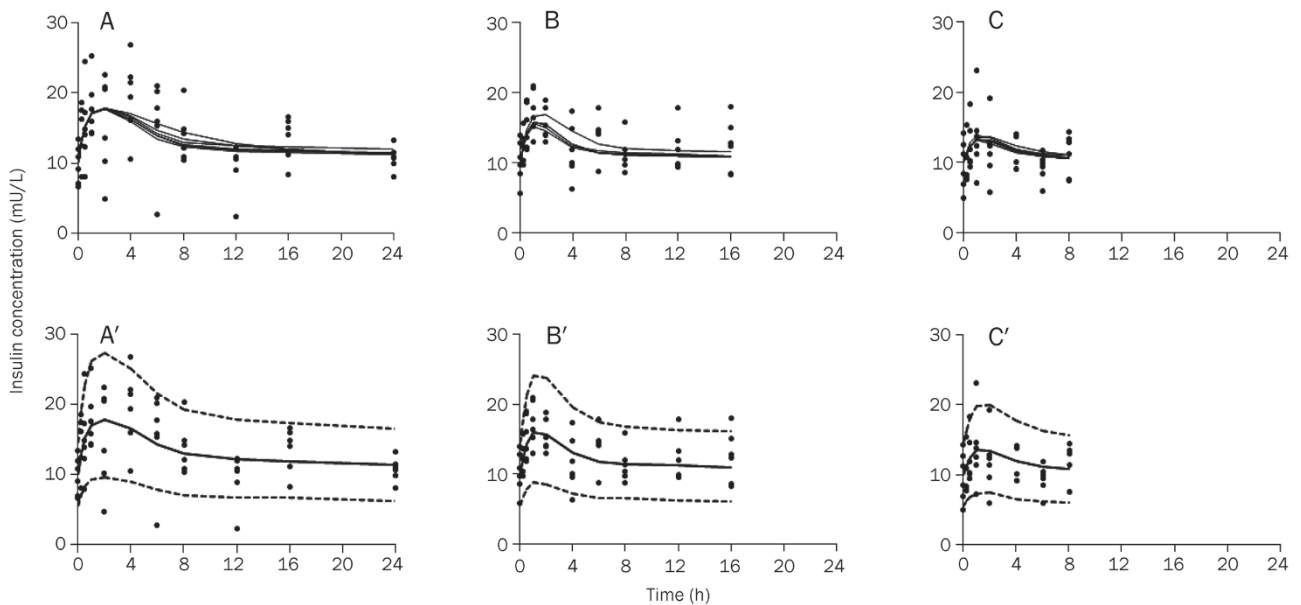


Figure 3. Observed and predicted serum insulin concentrations-time profiles after a single administration of exenatide at the dose of 210 (A), 42 (B), and 4.2 $\mu\text{g}/\text{kg}$ (C) in diabetic rats. The solid dots represent individual data from rats and the solid lines represent the model fit lines. Visual predictive check of serum insulin concentration-time profiles after single administrations of exenatide at the dose of 210 (A'), 42 (B'), and 4.2 $\mu\text{g}/\text{kg}$ (C'). The ranges between the dotted lines depict the 90% prediction intervals. The solid lines present the medians of simulated data. The solid dots are the observed concentrations.

from the difference in their t_{max} . Higher doses led to a longer lag time. VPC indicated that the model manifested acceptable predictability (Figure 3A'-3C'). However, some insulin con-

centrations less than 5 mU/L were overpredicted by the model (Figure 3A). 9.6% of measured insulin concentrations fell outside the 90% PI. The parameters for insulin turnover model

(Table 3) were estimated with good precision ($RSE\% \leq 30.0\%$, except for SC_{50} at 38.6%). The S_{m1} and SC_{50} are drug-specific parameters that characterize the effect of exenatide on insulin release, thus could be used for dose searching.

Table 3. Parameter estimates obtained from the insulin profiles after single sc injections of exenatide to diabetic rats in the PK/PD model.

Parameter*	Estimate (RSE%)	CV%
S_{m1}	0.822 (14.0)	28.3
SC_{50} ($\mu\text{g/L}$)	4.02 (38.6)	-
k_{in1} ($\text{mU}\cdot\text{L}^{-1}\cdot\text{h}^{-1}$)	21.3 (27.4)	-
k_{out1} (h^{-1})	2.11 (30.0)	-
Residual error		
σ_1 (Proportional, CV%)	27.1	
σ_2 (Additive, SD)	2.09 mU/L	

* S_{m1} , maximal insulinotropic response factor; SC_{50} , concentration for 50% of insulinotropic effect; k_{in1} , zero-order insulin production rate constant; k_{out1} , first-order insulin output rate constant; "-" refers to the CV% were fixed as 0.

The combined effect compartment/indirect response model adequately characterized the time course of *EOE* (Figure 4A-4C). Compared with its rapid absorption, exenatide caused a slow onset and marked reduction in *EOE* at all of the three dose levels. After administration, the maximal effects were achieved at 2, 2, and 2-4 h with the corresponding doses of 4.2, 42, and 210 $\mu\text{g/kg}$. The maximal *EOE* was 0.793 ± 0.077 , 0.668 ± 0.094 , and 0.550 ± 0.063 , respectively. The delay can

also be seen between the insulin and *EOE*. Plots of VPC of the final PK/PD model are shown in Figure 4A'-4C'. 14.1% of observed *EOE* fell outside the 90% PI. The PK/PD parameters estimated by the combined effect compartment/indirect response model are shown in Table 4. The RSE% estimated for the parameters were in a range from 9.58% to 43.6%. k_{e0} characterized the extent of delay. A smaller k_{e0} refers to a longer delay. I_m and S_{m2} characterized the capacity of insulin action. Only proportional residual error was included in the model, since the additive error was too small ($SD < 10^{-6}$).

Table 4. Parameter estimates obtained from the EFF profiles after single sc injections of exenatide to diabetic rats with PK/PD model.

Parameter*	Estimate (RSE%)	CV%
k_{e0} (h^{-1})	0.342 (43.6)	-
k_{outG} (h^{-1})	15.2 (10.3)	-
S_{m2} (L/mU)	0.0513 (27.9)	51.4
I_m (L/mU)	0.0381 (9.58)	16.0
Residual error		
σ_1 (Proportional, CV%)	7.92	
σ_2 (Additive, SD)	0 (Fix)	

* k_{e0} , first-order elimination rate constant from the effect compartment; k_{outG} , glucose output rate constant, $k_{inG} = k_{outG}$; S_{m2} , stimulatory factor of insulin on glucose disposal; I_m , inhibitory factor of insulin on glucose production; "-" refers to the CV% were fixed as 0.

Our model-predicted results are shown in Figure 5. In the confirmatory animal study, rats came from different batches

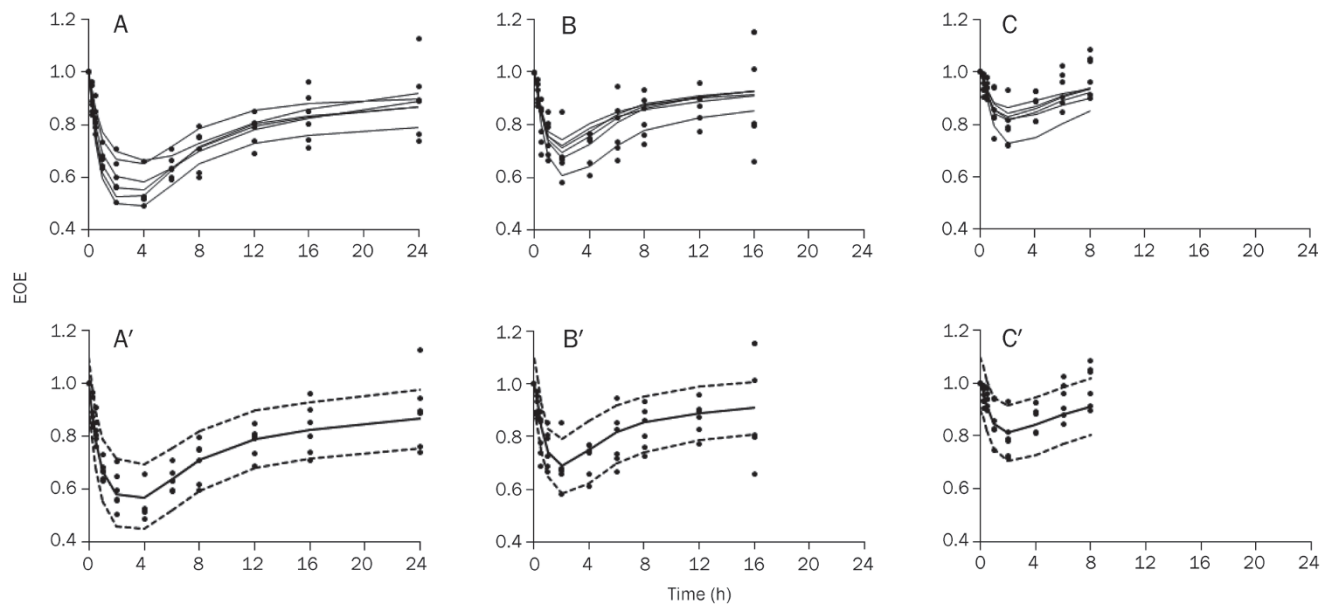


Figure 4. Observed and predicted *EOE*-time profiles after a single administration of exenatide at the dose of 210 (A), 42 (B), and 4.2 $\mu\text{g/kg}$ (C) in diabetic rats. The solid dots represent individual data from rats and the solid lines represent the model fit lines. (A-C). Visual predictive check of *EOE*-time profiles after single administrations of exenatide at the dose of 210 (A'), 42 (B'), and 4.2 $\mu\text{g/kg}$ (C'). The ranges between the dotted lines depict the 90% prediction intervals. The solid lines present the medians of simulated data. The solid dots are the observed values. (A'-C')

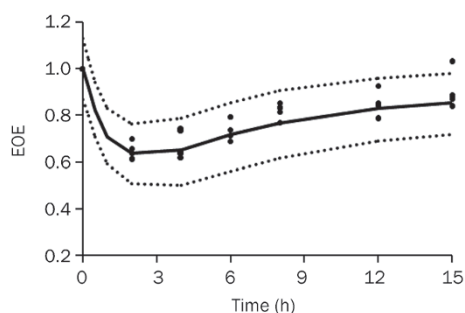


Figure 5. Observed EOE in the confirmatory animal study at the dose of 21 $\mu\text{g}/\text{rat}$, superimposed upon model simulation. Solid dots represent observations from individual rats, and the solid line is the predicted mean value. The ranges between the dashed lines depict the 90% prediction intervals.

and the sampling schedules were different. The model predictions agreed reasonably with the observations.

Discussion

It is reported that the hypoglycemic effect of exenatide is mediated by agonism of the GLP-1 receptor, which can enhance the secretion of insulin^[14]. Therefore, an indirect response model is appropriate to describe the insulinotropic effect of exenatide. An effect compartment model assumes a distributional delay to allow the drug to reach its site of action^[15]. Using an effect compartment model to describe the action of insulin on glucose has been reported previously^[16, 17], and many authors have employed indirect response model to describe insulin effects^[11, 18–20]. The results of comparison of indirect response models and effect compartment models for insulin in Yucatan minipigs indicated that indirect response model is a more appropriate approach for modeling the PK/PD of insulin than the effect compartment model^[21]. We deemed that distributional delay and indirect response mechanisms of action for insulin existed simultaneously, such that both effect compartment and indirect response model were integrated in our PK/PD model. Owing to fasting and single administration to diabetic rats, other gluco-regulatory mechanisms of exenatide were not included in this model: *eg*, slowing of gastric emptying to modulate nutrient absorption, reduction of food intake and body weight, increase of β -cell mass, and enhancement of β -cell function. To the best of our knowledge, this is the first report of using combined effect compartment/indirect response model to characterize the glucose-lowering effect of insulin via stimulating output and inhibiting input simultaneously.

High insulin concentrations exert strong glucose-lowering effects^[18]. Owing to the glucose-dependent enhancement of insulin secretion by exenatide, the insulin release stimulated by exenatide did not reach a high concentration. We believed that the insulin concentration was much less than the EC_{50} of insulin and there was a linear relationship between insulin and blood glucose. Therefore, linear factors (I_m and S_{m2}) were used to characterize the effects of insulin on glucose, instead

of using the E_{max} model.

Acute hyperglycemia, which was the result of pharmacologic stimulation of the GLP-1 receptor, was observed in three commonly used strains of rats (SD rats, Wistar Rats, and Long-Evans rats), and this type of response to GLP-1 receptor activation appeared to be specific for exenatide^[22]. A later study with Goto-Kakizak rats supported these findings^[11]. A target-mediated drug disposition model was used to characterize the pharmacokinetics of exenatide. Glucose turnover was described by an indirect response model, with insulin stimulating glucose disposition. Insulin turnover was characterized by an indirect response model with a precursor compartment. After administration, glucose initially declined because of enhanced insulin secretion, and then gradually increased because of the activation of the neural system by exenatide. The hyperglycemic action was modeled with increased hepatic glucose production. It is noteworthy that our estimated S_{m1} and SC_{50} (drug-specific parameters) are similar to their results^[11]. k_{in1} and k_{out1} (system-specific parameters) aren't comparable as a result of different groups of diabetic rats used, having different basal insulin values. However, acute hyperglycemia did not surface in the fat-fed, STZ-treated SD rats. In preliminary experiments, we found that frequent sampling (*eg*, sampling every 15 min) and taking a large volume of blood (*ie*, >0.5 mL) could elevate blood glucose and even counteract the glucose-lowering effect of exenatide. Therefore, the action of exenatide to elevate blood glucose in fat-fed, STZ-treated SD rats requires further study.

A physiological model of exenatide was developed to evaluate the effects on glucose-insulin homeostasis under hyperglycemic clamp conditions in healthy and type 2 diabetic subjects^[10]. A separate remote insulin compartment (act as an "effect compartment") and glucose-insulin feedback were employed into the pharmacodynamic model. Observed plasma glucose-insulin profiles were well characterized by this model. However, this model can't describe our data accurately, such as overpredicted EOE and smaller t_{max} values (time of maximal EOE). That may be related to the physiological differences between human and rat.

In conclusion, the combined effect compartment/indirect response model accounts for the insulin in blood and peripheral tissues (muscle and adipose); as well as the effects of insulin on blood glucose, such as control of cellular intake of glucose, and decreased gluconeogenesis and glycogenolysis. The hypoglycemic response of exenatide could be described and predicted accurately by the model. Though the data obtained from rat study is difficult to extrapolate to diabetic patients, the modeling procedure employed here may be useful in the future for investigating the pharmacokinetic and pharmacodynamic characteristics of other GLP-1 analogues in animals or human.

Acknowledgements

This work was supported by the Ministry of Science and Technology of China (Peking University New Drug Research & Development Platform, grant number 2009ZX09301-010).

Author contribution

Wei LU, Tian-yan ZHOU, and Xin-gang LI designed the research and wrote the paper; Xin-gang LI, Xuan ZHOU, and Ye CHEN performed the research; Xin-gang LI analyzed data and plotted figures; Liang LI and Yu-peng REN gave technical assistance.

References

- 1 Weyer C, Bogardus C, Mott DM, Pratley RE. The natural history of insulin secretory dysfunction and insulin resistance in the pathogenesis of type 2 diabetes mellitus. *J Clin Invest* 1999; 104: 787–94.
- 2 Barnett AH. New treatments in type 2 diabetes: a focus on the incretin-based therapies. *Clin Endocrinol (Oxf)* 2009; 70: 343–53.
- 3 Drucker DJ. Enhancing incretin action for the treatment of type 2 diabetes. *Diabetes Care* 2003; 26: 2929–40.
- 4 Parkes DG, Jodka C, Smith P, Nayak S, Rinehart L, Gingerich R, *et al*. Pharmacokinetic actions of exendin-4 in the rat: comparison with glucagon-like peptide-1. *Drug Develop Res* 2001; 53: 260–7.
- 5 Zander M, Madsbad S, Madsen JL, Holst JJ. Effect of 6-week course of glucagon-like peptide 1 on glycaemic control, insulin sensitivity, and beta-cell function in type 2 diabetes: a parallel-group study. *Lancet* 2002; 359: 824–30.
- 6 Parkes DG, Pittner R, Jodka C, Smith P, Young A. Insulinotropic actions of exendin-4 and glucagon-like peptide-1 *in vivo* and *in vitro*. *Metabolism* 2001; 50: 583–9.
- 7 Stoffers DA, Kieffer TJ, Hussain MA, Drucker DJ, Bonner-Weir S, Habener JF, *et al*. Insulinotropic glucagon-like peptide-1 agonists stimulate expression of homeodomain protein IDX-1 and increase islet size in mouse pancreas. *Diabetes* 2000; 49: 741–8.
- 8 Goke R, Fehmman HC, Linn T, Schmidt H, Krause M, Eng J, *et al*. Exendin-4 is a high potency agonist and truncated exendin-(9–39)-amide an antagonist at the glucagon-like peptide 1-(7–36)-amide receptor of insulin-secreting beta-cells. *J Biol Chem* 1993; 268: 19650–5.
- 9 Young AA, Gedulin BR, Bhavsar S, Bodkin N, Jodka C, Hansen B, *et al*. Glucose-lowering and insulin-sensitizing actions of exendin-4-studies in obese diabetic (ob/ob, db/db) mice, diabetic fatty Zucker rats, and diabetic rhesus monkeys (*Macaca mulatta*). *Diabetes* 1999; 48: 1026–34.
- 10 Mager DE, Abernethy DR, Egan JM, Elahi D. Exendin-4 pharmacodynamics: insights from the hyperglycemic clamp technique. *J Pharmacol Exp Ther* 2004; 311: 830–5.
- 11 Jusko WJ, Gao W. Pharmacokinetic and pharmacodynamic modeling of exendin-4 in type 2 diabetic goto-kakizaki rats. *J Pharmacol Exp Ther* 2011; 336: 881–90.
- 12 Xing XH, Zhang ZM, Hu XZ, Wu RQ, Xu C. Antidiabetic effects of *Artemisia sphaerocephala* Krasch. gum, a novel food additive in China, on streptozotocin-induced type 2 diabetic rats. *J Ethnopharmacol* 2009; 125: 410–6.
- 13 Gedulin BR, Smith PA, Jodka CM, Chen K, Bhavsar S, Nielsen LL, *et al*. Pharmacokinetics and pharmacodynamics of exenatide following alternate routes of administration. *Int J Pharm* 2008; 356: 231–8.
- 14 Schmitz O, Degn KB, Brock B, Juhl CB, Djurhuus CB, Grubert J, *et al*. Effect of intravenous infusion of exenatide (synthetic exendin-4) on glucose-dependent insulin secretion and counterregulation during hypoglycemia. *Diabetes* 2004; 53: 2397–403.
- 15 Sheiner LB, Stanski DR, Vozeh S, Miller RD, Ham J. Simultaneous modeling of pharmacokinetics and pharmacodynamics – application to D-tubocurarine. *Clin Pharmacol Ther* 1979; 25: 358–71.
- 16 Miyazaki M, Mukai H, Iwanaga K, Morimoto K, Kakemi M. Pharmacokinetic-pharmacodynamic modelling of human insulin: validity of pharmacological availability as a substitute for extent of bioavailability. *J Pharm Pharmacol* 2001; 53: 1235–46.
- 17 Woodworth JR, Howey DC, Bowsher RR. Establishment of time-action profiles for regular and Nph insulin using pharmacodynamic modeling. *Diabetes Care* 1994; 17: 64–9.
- 18 Gopalakrishnan M, Suarez S, Hickey AJ, Gobburu JV. Population pharmacokinetic-pharmacodynamic modeling of subcutaneous and pulmonary insulin in rats. *J Pharmacokinetic Pharmacodyn* 2005; 32: 485–500.
- 19 Agero H, Vicini P. Pharmacodynamics of NN2211, a novel long acting GLP-1 derivative. *Eur J Pharm Sci* 2003; 19: 141–50.
- 20 Kwon KI, Yun HY, Park HC, Kang W. Pharmacokinetic and pharmacodynamic modelling of the effects of glimepiride on insulin secretion and glucose lowering in healthy humans. *J Clin Pharm Ther* 2006; 31: 469–76.
- 21 Lin SS, Chien YW. Pharmacokinetic-pharmacodynamic modelling of insulin: comparison of indirect pharmacodynamic response with effect-compartment link models. *J Pharm Pharmacol* 2002; 54: 791–800.
- 22 Perez-Tilve D, Gonzalez-Matias L, Aulinger BA, Alvarez-Crespo M, Gil-Lozano M, Alvarez E, *et al*. Exendin-4 increases blood glucose levels acutely in rats by activation of the sympathetic nervous system. *Am J Physiol Endocrinol Metab* 2010; 298: E1088–96.